



Mechanical behaviour of a small-scale energy pile in saturated clay

Neda Yavari, Anh Minh A.M. Tang, Jean-Michel Pereira, Ghazi Hassen

► To cite this version:

Neda Yavari, Anh Minh A.M. Tang, Jean-Michel Pereira, Ghazi Hassen. Mechanical behaviour of a small-scale energy pile in saturated clay. *Geotechnique*, 2016, 66 (11), pp.878 - 887. 10.1680/jgeot.15.T.026 . hal-01515818

HAL Id: hal-01515818

<https://enpc.hal.science/hal-01515818>

Submitted on 3 May 2017

HAL is a multi-disciplinary open access archive for the deposit and dissemination of scientific research documents, whether they are published or not. The documents may come from teaching and research institutions in France or abroad, or from public or private research centers.

L'archive ouverte pluridisciplinaire **HAL**, est destinée au dépôt et à la diffusion de documents scientifiques de niveau recherche, publiés ou non, émanant des établissements d'enseignement et de recherche français ou étrangers, des laboratoires publics ou privés.

General Paper

Mechanical behaviour of a small-scale energy pile in saturated clay

Neda YAVARI, Anh Minh TANG, Jean-Michel PEREIRA, Ghazi HASSEN

Université Paris-Est, Laboratoire Navier (UMR CNRS 8205)

Corresponding author:

Dr. Anh Minh TANG

Université Paris-Est

Laboratoire Navier/Géotechnique (CERMES)

Ecole des Ponts ParisTech

6-8 avenue Blaise Pascal, Cité Descartes, Champs-sur-Marne

77455 Marne-la-Vallée

France

Email : anhminh.tang@enpc.fr

Phone : +33 1 64 15 35 63

Fax : +33 1 64 15 35 62

Abstract

The mechanical behaviour of an energy pile in saturated clay under thermo-mechanical loading was studied using a model pile. Axial load was first applied to the pile head in steps to determine the resistance of the pile under mechanical load. Afterwards, thermo-mechanical tests were performed by applying a heating/cooling cycle to the pile under constant axial load. The results show pile head heave during heating and settlement during cooling. Irreversible settlement was observed after the thermal cycles. Tests performed with various axial loads show that the thermal irreversible settlement is greater under a higher axial load.

Keywords: energy pile; small-scale model; saturated clay; creep; thermo-mechanical load.

Number of words: 4526

Number of figures: 11

Number of tables: 0

1. Introduction

Energy piles are usually used in thermo-active foundations to transfer the mechanical load of the building to the ground and to provide heat exchange between the same using a ground-source heat pump system (Brandl, 2006; de Moel *et al.*, 2010; Brandl, 2013; Mimouni & Laloui, 2014; Olgun *et al.*, 2014). Full-scale tests on the thermo-mechanical behaviour of energy piles show that the temperature changes can modify stress and strain in the piles (Laloui *et al.*, 2003; Bourne-Webb *et al.*, 2009; Amatya *et al.*, 2012; McCartney & Murphy, 2012; Murphy *et al.*, 2014; Wang *et al.*, 2014). Reduced-scale tests on energy piles in sand show sometimes contradictory trends: their shaft resistance decreased in capacity after thermal loading was introduced, after Wang *et al.* (2011), while Ng *et al.* (2015) found an increase of shaft resistance after heating. Stewart & McCartney (2013) found that the behaviour of a scale-model energy foundation tested in a geotechnical centrifuge during transient heating and cooling, agrees well with observation on full-scale end-bearing energy foundations reported in the literature. Numerical simulations reveal that the effect of temperature on the mechanical behaviour of the piles is mainly related to its thermal expansion/contraction (Laloui *et al.*, 2006; Péron *et al.*, 2011; Yavari *et al.*, 2014a).

However, it is well known that temperature might slightly modify the mechanical properties of saturated clay (Cekerevac & Laloui, 2004; Hueckel *et al.*, 2011; Hong *et al.*, 2013; Laloui *et al.*, 2014). In addition, irreversible volume change of soil induced by temperature variations (i.e. contraction of normally consolidated clay during heating, see Abuel-Naga *et al.* 2007) may have significant effects on the undrained shear strength of the soil, which may affect the foundation capacity during rapid loading. Also, heating could induce a small decrease of the shear strength of clay/concrete interface (Di Donna & Laloui, 2013; Murphy &

65 McCartney, 2014). As a result, beside the thermal expansion/contraction of the piles, other
66 phenomena should be considered as well when studying the mechanical behaviour of
67 energy piles in clay. Conducting full-scale tension load tests, Akrouch *et al.* (2014) found that
68 heating increases the creep rate of energy piles in high plasticity clay.

69 Beside direct effects of temperature changes, the impact of cyclic heating/cooling on energy
70 piles has been studied in various works. Ng *et al.* (2014) performed centrifuge modelling of
71 energy piles subjected to heating/cooling cycles in saturated clay under constant working
72 load and observed cumulating irreversible displacement (thermo-mechanical ratcheting)
73 over five thermal cycles. This irreversible settlement reached 3.8% of pile diameter in lightly
74 overconsolidated clay and 2.1% of pile diameter in heavily overconsolidated clay. Yavari *et*
75 *al.* (2014b) found that a heating/cooling cycle applied on a model pile inserted in dry sand
76 under constant axial load induced an irreversible displacement of around 2% of the pile
77 diameter. Amatya *et al.* (2012) analysed the results of several in situ experiments on energy
78 piles and concluded that heating/cooling cycles induce volume change of the energy piles,
79 which changes the pile-soil interaction. More precisely, the mobilized shaft resistance profile
80 of a mechanically loaded pile may undergo significant changes during thermal loading. After
81 Ng *et al.* (2014), beside the mobilisation of shaft resistance, thermo-mechanical ratcheting
82 can be attributed to a cumulating irreversible reduction of confining stress at the pile-soil
83 interface.

84 In the present work, the mechanical behaviour of energy piles in saturated clay is
85 investigated using a small-scale model. Heating/cooling cycles were performed under
86 various constant axial loads. The pile head axial displacement was monitored during these
87 thermo-mechanical loads.

2. Experimental method

The experimental setup is presented in Figure 1. This system is similar to that used in Yavari *et al.* (2014b). A pile was embedded in a container filled with saturated clay. The model pile was a closed-end aluminium tube with outer and inner diameters of 20 and 18 mm, respectively. The total length of the pile was 800 mm but only 600 mm was embedded in soil. The pile was coated with a layer of Fontainebleau sand (median grain size of 0.23 mm) by means of appropriate glue (Araldite). The added roughness will likely force failure to occur in the clay, which is softer, rather than at the interface.

The axial load applied to the pile head was controlled by the water level in the tank. A force sensor placed on the pile head measured pile head axial load. A displacement sensor monitored the pile head settlement. A heating/cooling circulating bath (cryostat) allowed the control of the pile temperature. Its internal reservoir was filled with water and connected to an aluminium U-shaped tube (2 mm internal diameter) inside the pile. The pile was filled with water to ensure the thermal transfer between the U-shaped tube and the pile. One temperature sensor was inserted inside the pile to monitor its temperature during the experiments. Note that the pile temperature will not be homogenous but it may be an appropriate assumption for the nature of the analysis in the present study.

Kaolin clay was used in this study. Its particle size distribution, obtained by laser diffraction method, is shown in Figure 2. It has a liquid limit of 57%, a plastic limit of 33%, and a particle density of 2.60 Mg/m³. More details about this material can be found in the work of Muhammed (2015). The soil powder was mixed with distilled water to a water content of 29% and then stored in hermetically sealed boxes for more than 24 h to ensure moisture homogenisation. Soil compaction started with three layers of 100, 100 and 50 mm. A

vibratory hammer was used to compact the soil to a dry density of 1.45 Mg/m^3 (that corresponds to a degree of saturation of 95% and a void ratio of 0.79). After the compaction of the first three layers, the pile was installed and the remaining soil was compacted around the pile by 100 mm thick layers. Attention was paid to ensure the homogeneity of soil next to the pile without touching the pile during soil compaction. Compaction layers are materialised using dashed lines in Figure 1. It should be noted that the average dry density of each compaction layer is controlled by the mass of soil used for compaction and the volume of the layer (thickness and diameter). Compacting the clay sample by several layers was chosen as an appropriate method to ensure its homogeneity prior to testing. Once compaction was finished, saturation was started by injecting water from the bottom of the container with a pressure of 20 kPa. To do so, the water tank was filled with water and its bottom was connected to the bottom of the soil container. At the end of the saturation, the level of water decrease and the final pressure was approximately 15 kPa. During this period, the water tank was blocked to avoid applying any force on the pile head. The soil surface was also covered with a thin layer of water and a plastic film to avoid water evaporation. This condition was maintained for 10 months until the estimated volume of water intake exceeded the initial air-filled pore volume. The soil was then assumed to be fully saturated. Measurement of the pile head displacement and visual inspection of the soil surface show that the soil surface did not move during saturation. Evaluation of the effects of saturation on the clay microstructure was not investigated. Note that Ng *et al.* (2014) consolidated kaolin clay slurry in order to obtain saturated clay sample for small-scale test but centrifuge was required to accelerate the consolidation process. In the present work, consolidation was not possible at 1-g condition. For this reason, compaction method was chosen to prepare the clay sample.

After saturation of the soil mass, the pile was first subjected to mechanical loading tests. Axial load was increased from 0 to 100 N, and then by increments of 50 N. Each increment was kept for 60 min. Loading was continued until failure, corresponding to a pile head settlement of 10% of the pile diameter (2 mm). Two mechanical tests, F1 and F2, were conducted using this loading procedure to check the repeatability of the experimental procedure. It should be noted that regarding the complexity of the compaction and saturation procedures, all the tests in this study were conducted on a single pile embedded at the centre of a single soil mass. This process was adopted following the work of Akrouch *et al.* (2014). An interval of two weeks between two subsequent mechanical tests was imposed to allow the equilibrium of stress state after each test. The initial states of the subsequent mechanical tests were then assumed to be similar.

After the mechanical tests, five thermo-mechanical tests were performed. Each test includes the following steps: (i) Increase of axial load to a given value which was maintained during the subsequent thermal cycle; (ii) Heating the pile from 22°C to 27°C; (iii) Cooling the pile to 22°C; (iv) Cooling the pile to 17°C; (v) Heating the pile to its initial temperature (22°C); (vi) Remove the axial load at 22°C. The pile temperature was maintained at 22°C until the subsequent test started. Each step took 120 min, except the last one, which was longer (800 min). Five thermo-mechanical tests, denoted by F3, F4, F5, F6 and F7, were performed at 100 N, 150 N, 200 N, 250 N and 300 N, respectively. This procedure allowed starting all the thermo-mechanical tests at the same pile temperature (22°C) and the duration of the last step (800 min) was assumed to be long enough to ensure the recovery of the system. That allows also performing one test per 24h and the five tests (F3-F7) in a week.

3. Experimental results

As all the tests were performed using a single soil mass and a single model pile, the global response of the soil/pile system is first examined via load settlement curves of the entire tests in Figure 3. The results show the permanent downward movement of the pile in the soil, which is more explicit under purely mechanical loading (tests F1 and F2). From the results of test F1 and considering 2 mm (10% of pile's outer diameter) as the pile settlement at failure, the pile's resistance can be estimated at 500-550 N. Test F2 was stopped intentionally before failure.

In Figure 4, the load-settlement curves of the thermo-mechanical tests (F3 to F7), which followed pile unloading in test F2, are shown at a larger scale. In each test, the pile response exhibits approximately the same stiffness during mechanical loading. The pile continues to settle during the applied thermal cycle under constant load. Unloading the pile leads to pile heave. The slope of the unloading branch is the same in all thermo-mechanical tests, except for test F4, which seems to be affected by a measurement problem. Also, the slope of the unloading branch in test F2 is identical to the corresponding phase of other tests.

The pile behaviour in each individual test was then investigated. The pile settlement was therefore zeroed (in the results analysis and not in the test) at the beginning of each test. The pile head displacement curves of all the tests are plotted versus the pile head axial load in Figure 5. The results relating to tests F3 to F7 are the pile response after the application of the mechanical load and just before starting thermal cycling. A good repeatability of the load-settlement curves can be observed, even when the figure is zoomed at a small range of settlement (from 0 to 0.06 mm).

The results of mechanical test F1 are presented in Figure 6, where the pile head settlement is plotted versus elapsed time for each loading step. That shows a quick settlement after the

load increase, followed by a stabilisation phase. As could be observed, for all the loading steps, the relationship between the settlement change and time (in a logarithmic scale) is linear under each loading step for $t = 2$ to 60 min. The creep rate could then be determined from the slope of each curve in Figure 5, based on the French standard (Afnor, 1999). Following this standard, for each loading step, the creep rate is calculated as the change of pile head displacement between 2 and 60 min (of elapsed time) divided by $\log(60/2)$. In Figure 7, the creep rate is plotted versus the axial load for all the tests. Note that in tests F1 and F2, the same procedure was followed (loading by steps), while in tests F3-F7, the target axial load was applied in one step. In spite of these different procedures, the relationships between the creep rate and the axial load are found to be similar in all tests; the creep rate increases quickly when the axial load exceeds 400 N. The fact that this rate depends only on the axial load and that it is independent of the loading path proves that it corresponds solely to creep and not to soil consolidation. After Edil & Mochtar (1988), the time-dependent displacement of a pile inserted in clay under a constant axial load is attributed primarily to creep of the pile-soil interface (slip) and shear creep of the soil surrounding the pile.

The load and the temperature of the pile measured in tests F3 to F7 are plotted in Figure 8. As explained above, from its initial temperature (around 22°C) after mechanical loading, the pile was heated to 27°C, cooled to 22°C, then cooled to 17°C, and finally heated to 22°C. The results show that the duration of each step (120 min) is long enough to bring the pile's temperature to the target value. During these heating/cooling steps, the pile head axial load was maintained constant (from $t = 0$ to 600 min) by keeping the same water level in the water tank (see Figure 1). However the load measured by the force sensor appeared not to be perfectly constant. This blip in load reading can be explained by the small friction

between the rod, which transfers the water tank load to the pile head, and the frame that supports it. Heating the pile induces a pile head heave. In this case, the measured load corresponds to the water tank load plus the friction force. Inversely, cooling the pile induces a pile head settlement, and the load measured corresponds to the water tank load minus the friction force. These changes, in the order of a few Newtons, can be ignored in this study.

The results of tests F3-F7 are shown in Figure 9. Pile head settlement versus elapsed time is shown in Figure 9(a, c, e, g, i) for the whole test including mechanical loading, thermal cycle, and mechanical unloading. The pile settles under the mechanical load in the first 120 min of the test. It begins to heave while being heated from 22°C to 27°C. It settles during the subsequent cooling down to 17°C and heaves again during the last heating which increases the temperature back to 22°C. The final unloading (when the axial load is removed at t = 600 min) induces a pile head heave. The time allocated to each thermal stage (120 min) may not be suitable for a relatively low-permeability material but the results show that the pile head displacement seems reached equilibrium at the end of each stage.

The change of pile head settlement versus change of temperature during the thermal cycle (between 120 min and 600 min in Figure 9a, c, e, g and i) is exhibited in Figure 9b, d, f, h, and j. The thermal expansion curve of an aluminium pile, having a fixed toe and being free to expand/contract in other directions, is also plotted. Its slope is equal to the linear thermal expansion coefficient of aluminium ($23 \times 10^{-6}/^{\circ}\text{C}$). This representation is similar to that used by Kalantidou *et al.* (2012), Yavari *et al.* (2014), and Ng *et al.* (2014). The experimental results show that the pile reacts immediately to temperature change and heaves with the first heating; however its heave is smaller than that of the pile thermal expansion curve. It

settles when it is cooled. Under 100 N of axial load (Fig 8b), the slope of the cooling branch is close to that of the heating. This slope seems higher at higher pile head loads and looks similar to the pile thermal expansion curve under 300 N (Fig 8f). The pile heaves during the second heating phase; the slopes of the two heating branches are almost equal.

For further analysis of the pile displacement, the axial displacement distribution was plotted for each thermo-mechanical test (similar analysis have been done by Di Donna & Laloui, 2015; Rotta Loria *et al.*, 2015). The end of the mechanical loading (start of 1st heating) was taken as the reference, with an axial displacement equal to zero along the pile. The first heating induced a pile head heave (in the figure, the axial displacement at 0 mm depth is taken equal to the measured pile head heave at the end of the first heating). The thermal expansion strain of the pile during this heating of 5°C is equal to $5 \times 23 \times 10^{-6} = 115 \times 10^{-6}$, where 23×10^{-6} is the coefficient of thermal expansion of the pile. The stress change during heating along the pile was not measured in this study. However, as the pile head load was fixed during heating, the axial load along the pile can be reasonably assumed to be smaller than 20% of the maximal load (300 N). This assumption can be justified from other tests under similar conditions, *i.e.* heating a floating pile under constant pile head load (Bourne-Webb *et al.*, 2009; Ng *et al.*, 2015). The maximal axial stress change (20% of the maximal load divided by the pile section) along the pile during heating can then be estimated as $20\% \times 300 / (0.01 \times 0.01 \times 3.14) = 19 \times 10^4$ Pa. That corresponds to an axial strain (axial stress divided by the pile equivalent Young modulus) of $19 \times 10^4 / 13 \times 10^9 = 15 \times 10^{-6}$ (where 13×10^9 Pa is the equivalent Young modulus of the pile following Yavari *et al.*, 2014a). This estimation shows that the axial displacement along the pile related to the stress change during heating can be ignored compared to the thermal expansion. The distribution of the axial displacement along the pile can then be estimated from the pile head displacement

(measured) and the pile thermal expansion calculated (see Figure 10). The results show that the pile toe settles during the first heating. The subsequent cooling induces heave at the pile toe except the case of the highest pile head load (F7), where settlement of the pile toe was observed. In addition, the higher the pile head load, the lower the pile toe's heave during cooling. The second heating induces a settlement at the pile toe for all the tests. These trends are similar to that observed by Pasten & Santamarina (2014), using numerical modelling.

In Figure 11, the pile head settlement induced by thermal cycling (between 120 min and 600 min) is plotted versus the applied pile head axial load for each test. From the creep rate, shown in Figure 6, the settlement related to the creep during this period can be estimated. Note that Cui *et al.* (2009) showed that the temperature can significantly influence the time dependent behaviour of clay but their tests were performed in a large range of temperature (from 25°C to 80°C). In the present work, the temperature change is much smaller (from 17°C to 27°C) and the pile head settlement related to creep (smaller than 0.005 mm for each period) is small compared to that related to the mechanical loading (see Figure 11). As a consequence, effects of temperature on creep settlement can be ignored. The settlement directly related to the thermal cycle can then be estimated: corrected value is the measured value minus the creep value (calculated from isothermal mechanical tests, see Figure 7). The results show that the settlement related to the thermal cycle is higher when the pile is subjected to a higher axial load.

4. Discussion

The results obtained on the mechanical loading part (Figures 5 and 7) show a good repeatability between the tests. The same settlement curve of the pile in all tests indicates

that the behaviour of the pile in one test is independent of the previous one. That suggests that the soil/pile system could have retrieved its initial equilibrium condition prior to the subsequent test. Actually, the pile has been loaded to failure during test F1 (Figure 3). For the subsequent test (F2), the pile shaft resistance would decrease due to the possible softening of the shear behaviour at the clay/pile interface (see Di Donna *et al.* 2016; Yavari *et al.* 2016). On the contrary, the pile toe resistance would increase if the clay consolidates after test F1. On one hand, the two mechanisms have opposite effects on the pile response; on the other hand, they could be negligible (because the clay has been already well compacted and the softening observed on a similar material by Yavari *et al.* 2016 is quite small under low stresses). That would explain why the mechanical response of the pile during test F2 is quite similar to that during test F1 (see Figure 5), suggesting that the waiting stage after failure test is sufficient for the clay to recover its initial mechanical properties. The choice of performing various tests in a unique mass of saturated clay can thus be considered as an appropriate one.

It should be noted that the irreversible settlement observed during the thermal cycle is larger at a higher axial load. While testing dry sand, Kalantidou *et al.* (2012) and Yavari *et al.* (2014b) found that the effect of thermal cycle under constant axial load was reversible under low loads (smaller than 30% of the pile resistance) and irreversible under high loads. In the present work, where tests were performed within a wide range of axial load (from 20% to 60% of the pile's resistance), irreversible settlement is observed even at low loads (100 N corresponds to less than 20% of the pile resistance, which is between 500 and 550 N). Ng *et al.* (2014) have also observed irreversible settlement after thermal cycles under constant load at 40% of the pile's resistance. However, in the work of Ng *et al.* (2014), thermo-mechanical ratcheting was observed to level off after few thermal cycles. In the present

work, only one thermal cycle was applied and such phenomenon could not be observed.

Concerning accumulated thermal displacement, Ng *et al.* (2014) obtained 2.1% and 3.8% of pile diameter after five cycles. In the present work, the irreversible thermal settlement obtained after one cycle was smaller than 0.5% of the pile diameter, which is in agreement with the work of Ng *et al.* (2014).

Beside experimental works, irreversible settlement of energy piles subjected to thermal cycles has also been investigated through numerical modelling. Suryatriyastuti *et al.* (2014) used a load transfer approach to study the cyclic behaviour of energy pile and found that thermo-mechanical ratcheting observed under thermal cycle could be predicted by considering a cyclic strain hardening/softening mechanism at the soil/pile interface. However, in the work of Pasten & Santamarina (2014), the main features of energy piles subjected to static load and thermal cycles (i.e. irreversible settlement after thermal cycles and displacement accumulation depending on the static factor of safety) were reproduced by numerical simulations without considering the cyclic strain hardening/softening mechanism. Actually, the authors explained the irreversible settlement by the decrease of mobilised shaft shear stress with thermal cycles. Saggu & Chakraborty (2015) simulated the cyclic thermo-mechanical behaviour of a floating energy pile in sand, and found an irreversible settlement only for the first heating/cooling cycle. The subsequent cycles induce an irreversible uplift of the pile.

In the present work, only one heating/cooling cycle was applied for each loading step. Thermo-mechanical ratcheting was observed for all the tests. In addition, this settlement is higher at a higher mechanical load. The mechanisms by which thermal cycles affect the pile behaviour can be explained from the profile of axial displacement shown in Figure 10.

Actually, after the mechanical loading, the first heating induces a pile expansion. This latter corresponds to a pile head heave (that was measured from the experiments) and a pile toe settlement. The pile toe settlement is induced by the reduction of the pile shaft resistance, which increases the load transfer to the pile toe (see Pasten & Santamarina, 2014). The subsequent cooling induces a pile contraction, which induces a pile head settlement (measured experimentally) and a pile toe heave (except for the case at high load, F7, where a pile toe settlement was expected). It should be also noted that the pile toe heave during cooling is lower at a higher mechanical load. Finally, the second heating, which brings the pile back to its initial temperature, induces again a pile toe settlement. The total pile toe settlement after the thermal cycle is positive and higher at a higher mechanical load. To explain these results, the pile toe settlement can be attributed to two mechanisms: (i) the compression of the clay below the pile toe; (ii) the displacement of the pile related to shearing of the clay surrounding the pile toe. If the first mechanism can be expected to be almost reversible, the second one is most likely irreversible. The observed thermo-mechanical ratcheting can then be attributed to the second mechanism (shearing of the clay surrounding the pile toe).

The thermally induced irreversible settlement could become significant in the design of energy piles in saturated clay. When all the piles of the foundation are equipped with the heat exchanger system, additional settlement of the foundation can be expected with seasonal temperature change of piles. When only a part of foundation piles is equipped with the heat exchanger system, cycles of temperature applied to these piles would reduce progressively their axial load while the axial load in the non-equipped piles increases, thus leading to redistributions of loads among the different piles.

5. Conclusion

Thermo-mechanical loading was applied to a model pile in saturated clay. The pile head axial load, displacement and temperature were monitored. Analysis of the experimental results shows that:

- Under mechanical loading, the creep rate (of the pile head displacement) increases as the pile head load approaches to pile ultimate resistance but remains negligible at low pile head load.
- Under a constant pile head axial load, heating the pile induces pile head heave while cooling induces settlement. This behaviour is mainly related to the thermal expansion/contraction of the pile.
- Irreversible settlement of the pile head is observed after the heating/cooling cycle under constant pile head axial load. This settlement is larger under higher axial loads, and is much more significant than that due to creep under isothermal conditions.

The findings of this study, observed on a model pile, would be helpful when considering the long-term mechanical behaviour in the design of energy piles in saturated clay. Actually, seasonal piles temperature change could induce additional settlement of the foundation or redistribution of foundation load on the piles.

6. Acknowledgement

The authors would like to express their great appreciation to the French National Research Agency for funding the present study, which is part of the project PiNRJ "Geotechnical aspects of foundation energy piles" – ANR 2010 JCJC 0908 01.

7. References

- Abuel-Naga, H.M., Bergado, D.T., Bouazza, A. & Ramana, G.V. (2007). Volume change behaviour of saturated clays under drained heating conditions : experimental results and constitutive modeling. *Canadian Geotechnical Journal* **44**, 942 – 956.
- AFNOR (1999). Essai statique de pieu sous effort axial. NF P 94-150.
- Akrouch, G., Sánchez, M. & Briaud, J. (2014). Thermo-mechanical behavior of energy piles in high plasticity clays. *Acta Geotechnica* **6**, 503–519.
- Amatya, B. L., Soga, K., Bourne-Webb, P. J., Amis, T. & Laloui, L. (2012). Thermo-mechanical behaviour of energy piles. *Géotechnique* **62**, No. 6, 503–519.
- Bourne-Webb, P. J., Amatya, B., Soga, K., Amis, T., Davidson, C. & Payne, P. (2009). Energy pile test at Lambeth College, London: geotechnical and thermodynamic aspects of pile response to heat cycles. *Géotechnique* **59** No. 3, 237–248.
- Brandl, H. (2006). Energy foundations and other thermo-active ground structures. *Géotechnique* **56**, No. 2, 81–122.
- Brandl, H. (2013). Thermo-active ground-source structures for heating and cooling. *Procedia Engineering* **57**, 9–18.
- Cekerevac, C. & Laloui, L. (2004). Experimental study of thermal effects on the mechanical behaviour of a clay. *International Journal for Numerical and Analytical Methods in Geomechanics* **28**, 209–228.
- Cui, Y.J., Le, T.T., Tang, A.M., Delage, P. & Li, X.L. (2009). Investigating the time-dependent behaviour of Boom clay under thermomechanical loading. *Géotechnique* **59**, No. 4, 319 – 329.

- De Moel, M., Bach, P. M., Bouazza, A., Singh, R. M. & Sun, J. O. (2010). Technological advances and applications of geothermal energy pile foundations and their feasibility in Australia. *Renewable and Sustainable Energy Reviews* **14**, No. 9, 2683–2696.
- Di Donna, A & Laloui, L. (2013). Advancements in the Geotechnical Design of Energy Piles. *International Workshop on Geomechanics and Energy*, (November 2013), 26–28.
- Di Donna, A. & Laloui, L. (2015). Numerical analysis of the geotechnical behaviour of energy piles. *Int. J. Numer. Anal. Meth. Geomech.* **39**, 861 – 888.
- Di Donna, A., Ferrari, A. & Laloui, L. (2016). Experimental investigation of the soil-concrete interface: physical mechanisms, cyclic mobilisation and behaviour at different temperatures. *Canadian Geotechnical Journal* (doi: 10.1139/cgj-2015-0294).
- Edil, T.B. & Mochtar, I.B. (1988). Creep response of model pile in clay. *Journal of Geotechnical Engineering* **114**, No. 11, 1245 – 1260.
- Hong, P. Y., Pereira, J. M., Tang, A. M. & Cui, Y. J. (2013). On some advanced thermo-mechanical models for saturated clays. *International Journal for Numerical and Analytical Methods in Geomechanics* **37**, No. 17, 2952–2971.
- Hueckel, T., Francois, B. & Laloui, L. (2011). Temperature-dependent internal friction of clay in a cylindrical heat source problem. *Géotechnique*, **61**, No. 10, 831–844.
- Kalantidou, A., Tang, A. M., Pereira, J.-M. & Hassen, G. (2012). Preliminary study on the mechanical behaviour of heat exchanger pile in physical model. *Géotechnique* **62**, No. 11, 1047–1051.

- Laloui, L., Moreni, M. & Vulliet, L. (2003). Comportement d'un pieu bi-fonction, fondation et échangeur de chaleur. *Canadian Geotechnical Journal* **40**, No. 2, 388–402.
- Laloui, L., Nuth, M. & Vulliet, L. (2006). Experimental and numerical investigations of the behaviour of a heat exchanger pile. *International Journal for Numerical and Analytical Methods in Geomechanics* **30**, No. 8, 763–781.
- Laloui, L., Olgun, C. G., Sutman, M., McCartney, J. S., Coccia, C. J., Abuel-Naga, H. M. & Bowers, G. A. (2014). Issues involved with thermoactive geotechnical systems: characterization of thermomechanical soil behavior and soil-structure interface behavior. *DFI Journal: The Journal of the Deep Foundations Institute* **8**, No. 2, 108–120.
- McCartney, J. S. & Murphy, K. D. (2012). Strain Distributions in Full-Scale Energy Foundations (DFI Young Professor Paper Competition 2012). *DFI Journal: The Journal of the Deep Foundations Institute* **6**, No. 2, 26–38.
- Mimouni, T. & Laloui, L. (2014). Towards a secure basis for the design of geothermal piles. *Acta Geotechnica* **9**, 355 – 366.
- Muhammed, R.D. (2015). *Etude en chambre d'étalonnage du frottement sol-pieu sous grands nombres de cycles. Applications au calcul des fondations profondes dans les sols fins saturés*. PhD thesis of Université Pierre Marie Curie, 204 pages.
- Murphy, K. D. & McCartney, J. S. (2014). Thermal Borehole Shear Device. *Geotechnical Testing Journal* **37**, No. 6, 20140009.
- Murphy, K. D., McCartney, J. S. & Henry, K. S. (2014). Evaluation of thermo-mechanical and thermal behavior of full-scale energy foundations. *Acta Geotechnica* **10**, 179-195.

- Ng, C. W. W., Shi, C., Gunawan, A. & Laloui, L. (2014). Centrifuge modelling of energy piles subjected to heating and cooling cycles in clay. *Géotechnique Letters* **4**, 310 –316.
- Ng, C. W. W., Shi, C., Gunawan, A., Laloui, L. & Liu, H.L. (2015). Centrifuge modelling of heating effects on energy pile performance in saturated sand. *Can. Geotech. J.* **52**, 1045 – 1057.
- Olgun, C.G., Ozudogru, T.Y., Abdelaziz, S.L. & Senol, A. (2014). Long-term performance of heat exchanger piles. *Acta Geotechnica* **10**, No. 5, 553 – 569.
- Pasten, C. & Santamarina, C. (2014). Thermally Induced Long-Term Displacement of Thermoactive Piles. *J. Geotech. Geoenviron. Eng.*, **140**(5): 06014003
- Péron, H., Knellwolf, C. & Laloui, L. (2011). A method for the geotechnical design of heat exchanger piles. *Geo-Frontiers 2011*, 470–479.
- Rotta Loria, A.F., Gunawan, A., Shi, C., Laloui, L. & Ng, W.W.C. (2015). Numerical modelling of energy piles in saturated sand subjected to thermo-mechanical loads. *Geomechanics for Energy and the Environment* **1**, 1 – 15.
- Saggu, R. & Chakraborty, T. (2015). Cyclic Thermo-Mechanical Analysis of Energy Piles in Sand. *Geotech Geol Eng* **33**, 321–342
- Stewart, M.A. & McCartney, J.S. (2013). Centrifuge modelling of soil-structure interaction in energy foundations. *Journal of Geotechnical and Geoenvironmental Engineering* **140**, No. 4, 04013044.
- Suryatriyastuti, M.E., Mroueh, H. & Burlon, B., 2014. A load transfer approach for studying the cyclic behavior of thermo-active piles. *Computers & Geotechnics* **55**, 378 – 391.

- Wang, B., Bouazza, A. & Haberfield, C. (2011). Preliminary observation from laboratory scale model geothermal pile subjected to thermo-mechanical loading. *Geo-Frontiers 2011*, 430 – 439.
- Wang, B., Bouazza, A., Singh, R. M., Haberfield, C., Barry-macaulay, D. & Baycan, S. (2014). Posttemperature Effects on Shaft Capacity of a Full-Scale Geothermal Energy Pile. *Journal of Geotechnical and Geoenvironmental Engineering* **141**, No. 4, 04014125.
- Yavari, N., Tang, A. M., Pereira, J.-M. & Hassen, G. (2014a). A simple method for numerical modelling of energy pile's mechanical behaviour. *Géotechnique Letters* **4**, 119–124.
- Yavari, N., Tang, A. M., Pereira, J.-M. & Hassen, G. (2014b). Experimental study on the mechanical behaviour of a heat exchanger pile using physical modelling. *Acta Geotechnica* **9**, No. 3, 385 – 398.
- Yavari, N., Tang, A. M., Pereira, J.-M. & Hassen, G. (2016). Effect of temperature on the shear strength of soils and soil/structure interface. *Canadian Geotechnical Journal* (doi: 10.1139/cgj-2015-0355)

467 **List of captions**

468 Figure 1. Experimental set-up

469 Figure 2. Grain size distribution curve of kaolin clay

470 Figure 3. Pile load-settlement curve obtained through 7 successive tests F1 to F7

471 Figure 4. Pile load-settlement curve obtained through tests F3 to F7

472 Figure 5. Load-settlement curves for the mechanical phase

473 Figure 6. Results of test F1 – Pile head settlement versus elapsed time for each loading step

474 Figure 7. Creep rate versus axial load for the mechanical phase

475 Figure 8. Axial load and temperature of the pile in tests: (a) F3; (b) F4; (c) F5; (d) F6; (e) F7.

476 Figure 9. Results of tests F3-F7 for the thermal phase – Pile head settlement and pile temperature
477 change: (a, b) F3; (c, d) F4; (e, f) F5; (g, h) F6; (i, j) F7.

478 Figure 10. Results of tests F3-F7 for the thermal phase - Axial displacement along the pile: (a) F3; (b)
479 F4; (c) F5; (d) F6; (e) F7.

480 Figure 11. Results of tests F3-F7 for the thermal phase - Pile head settlement versus pile head axial
481 load

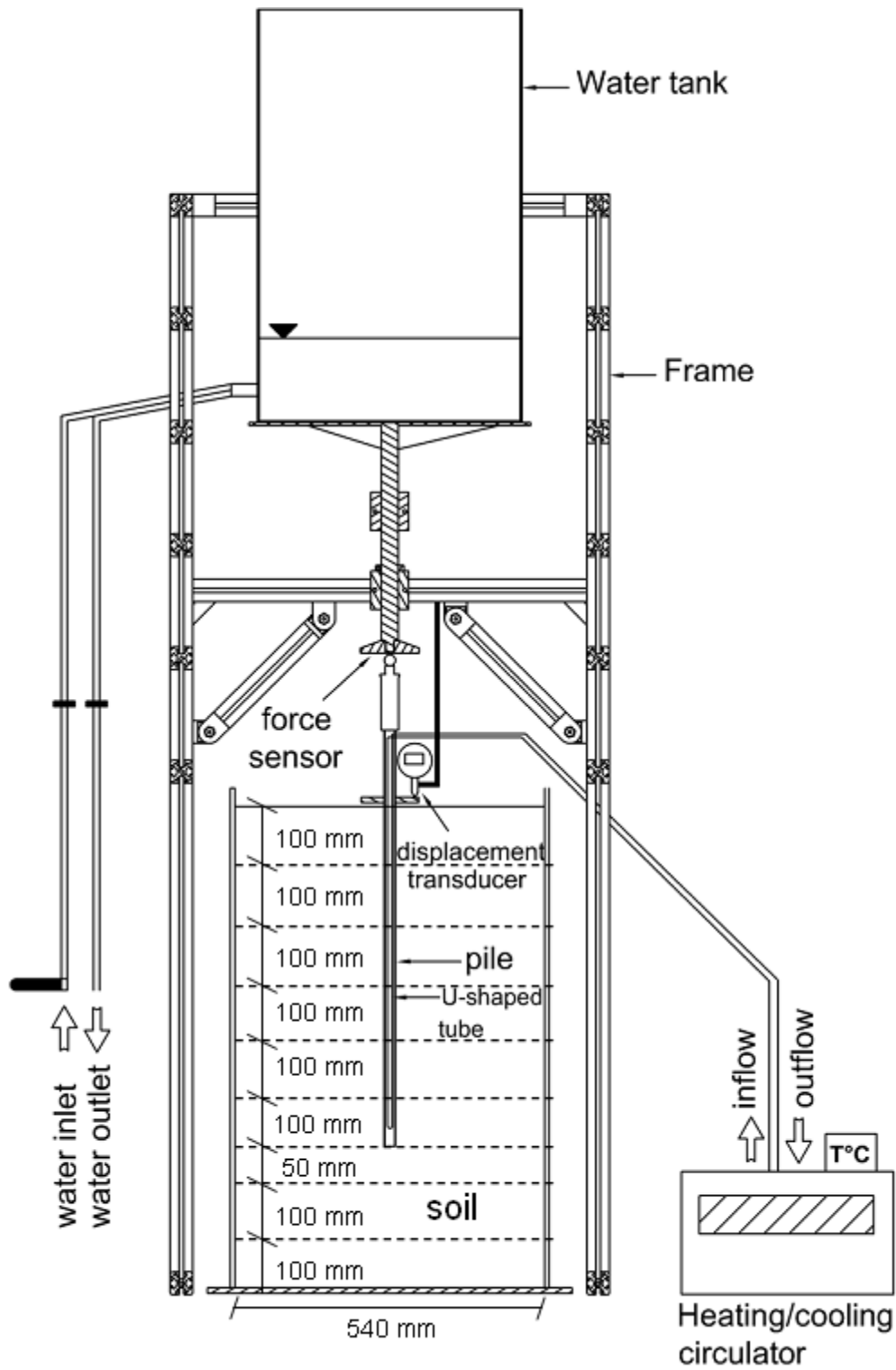


Figure 1. Experimental set-up

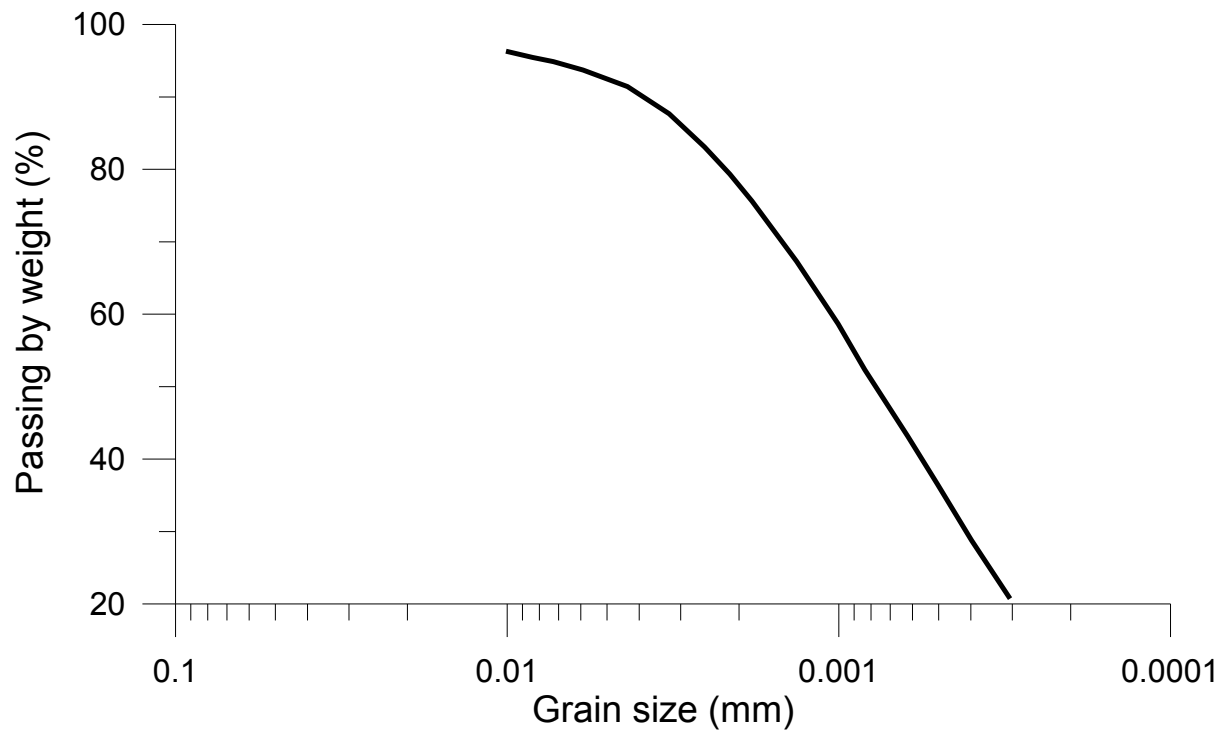


Figure 2. Grain size distribution curve of kaolin clay

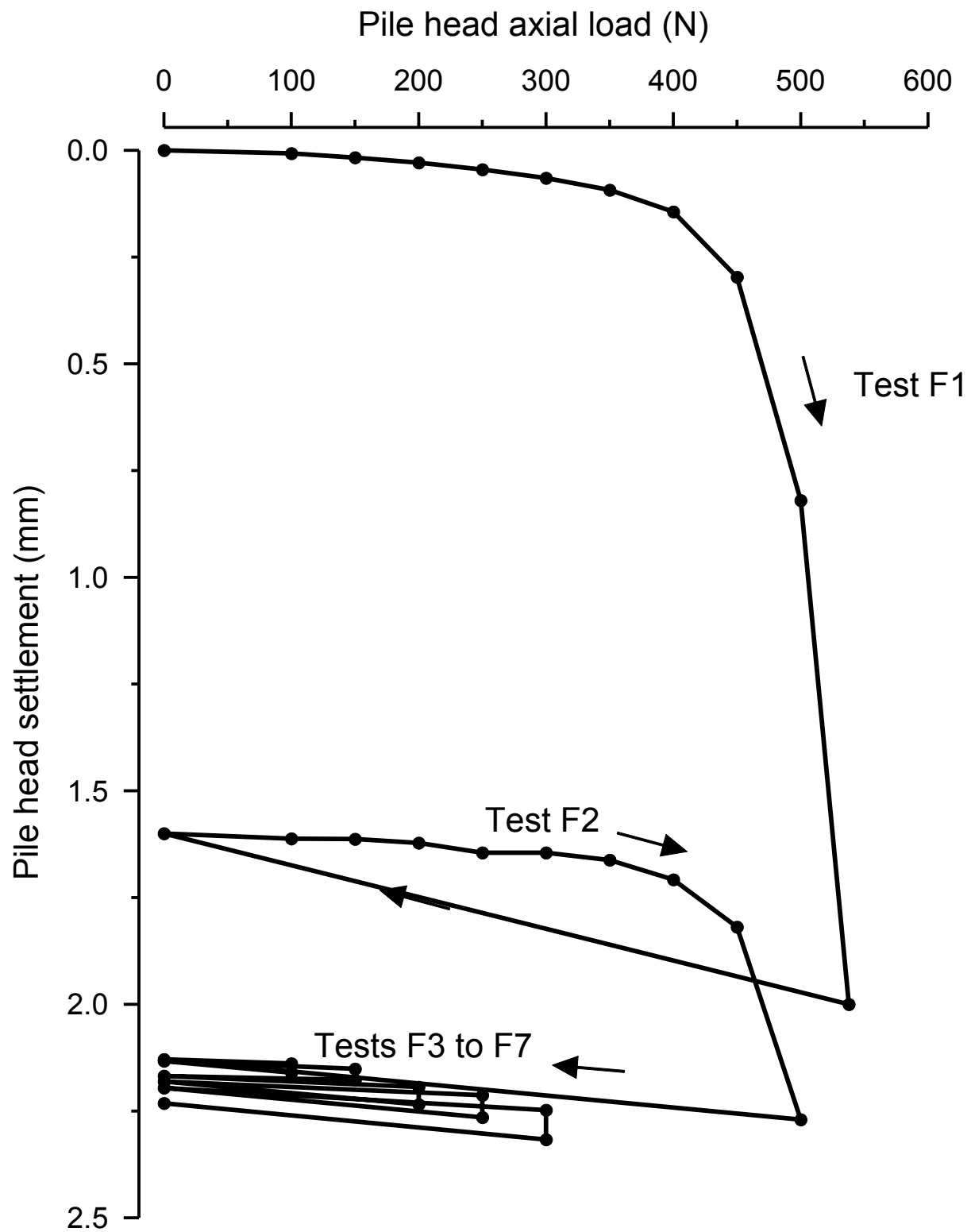


Figure 3. Pile load-settlement curve obtained through 7 successive tests F1 to F7

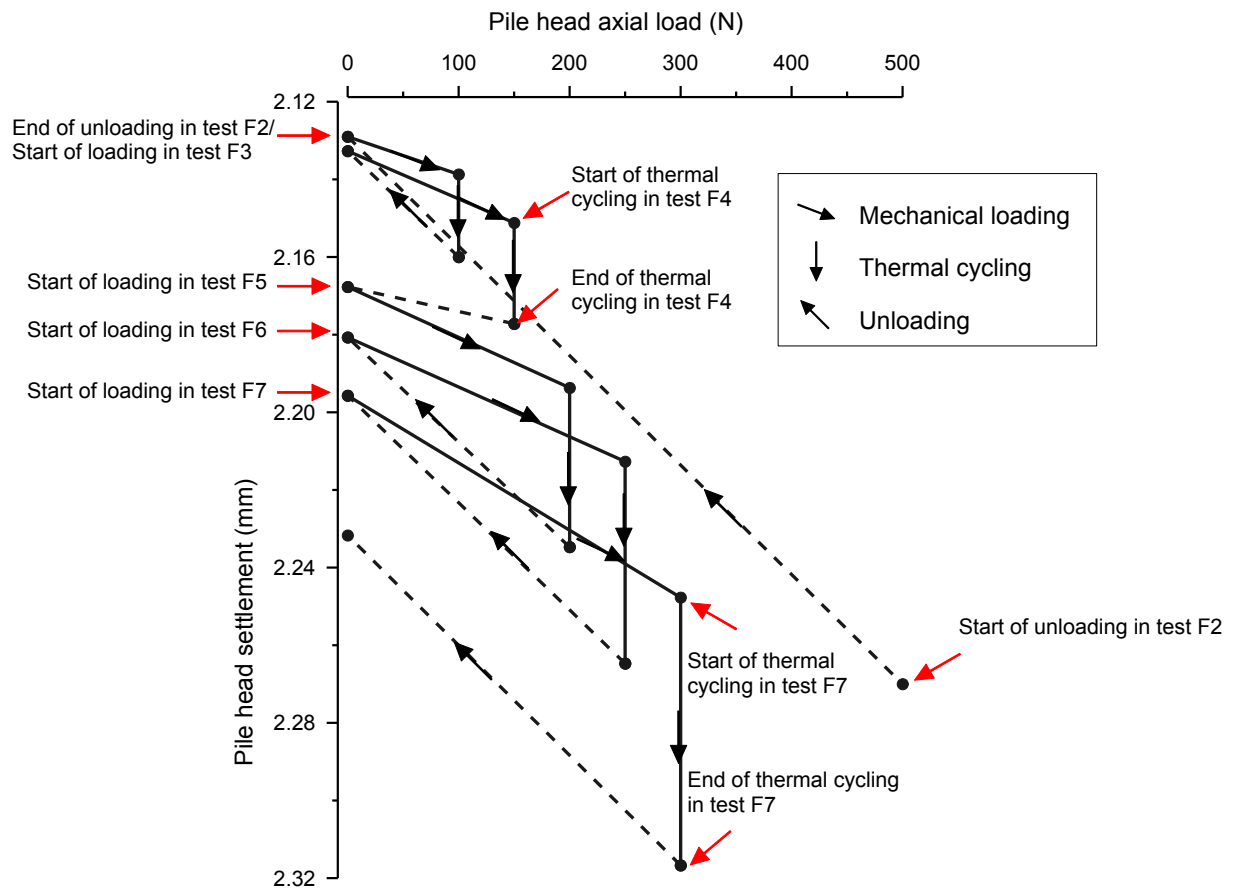


Figure 4. Pile load-settlement curve obtained through tests F3 to F7

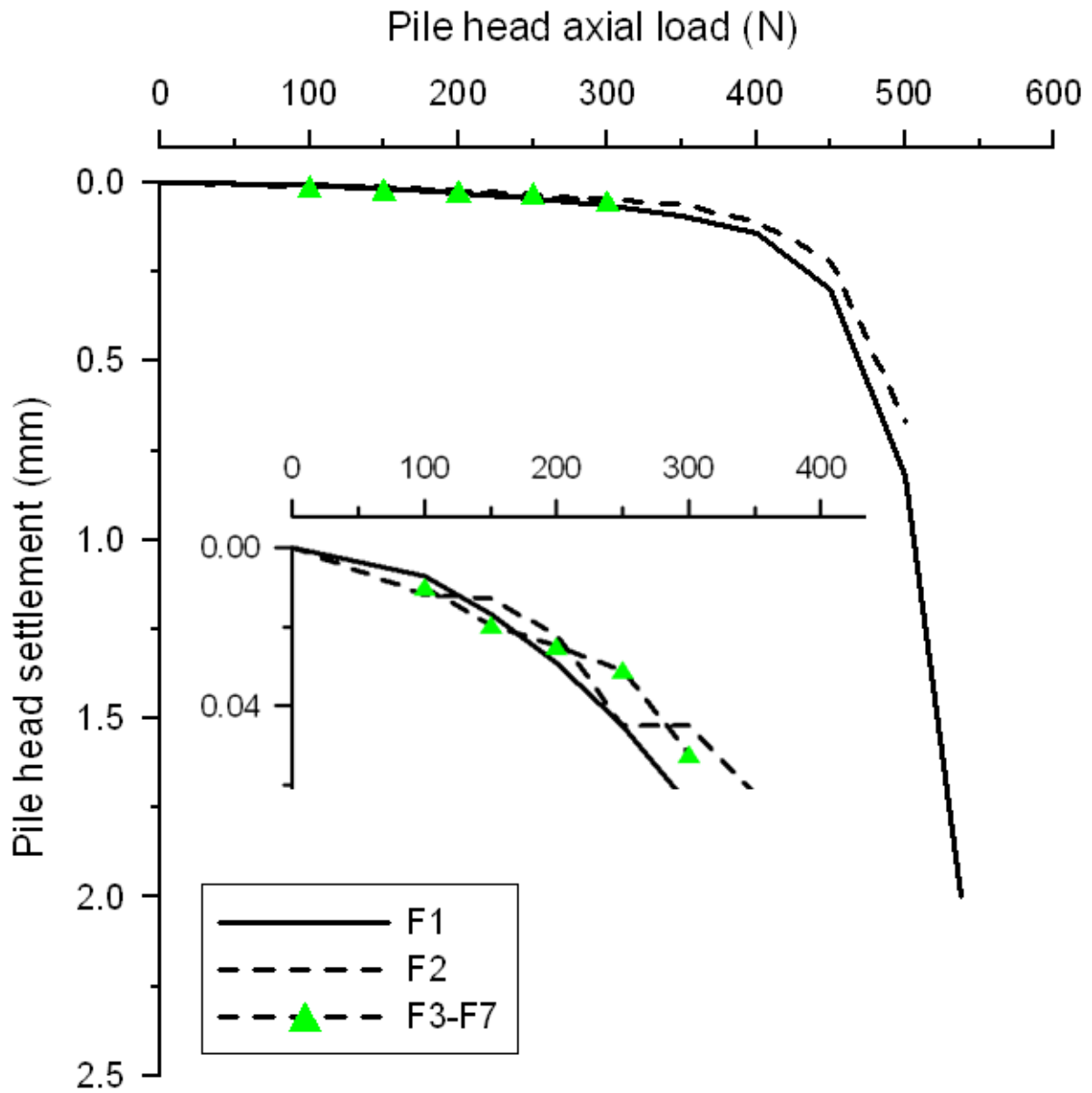


Figure 5. Load-settlement curves for the mechanical phase

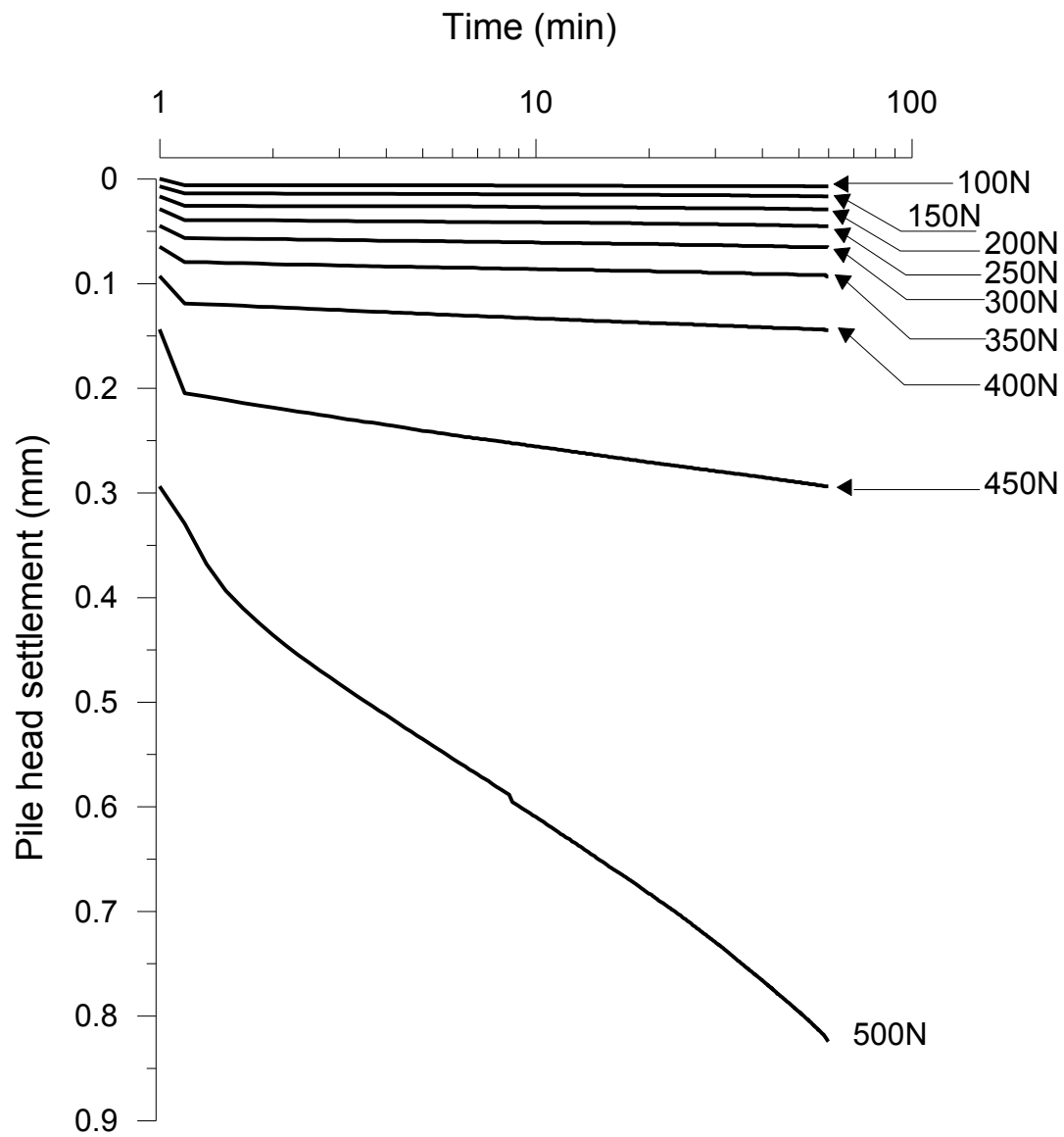


Figure 6. Results of test F1 – Pile head settlement versus elapsed time for each loading step

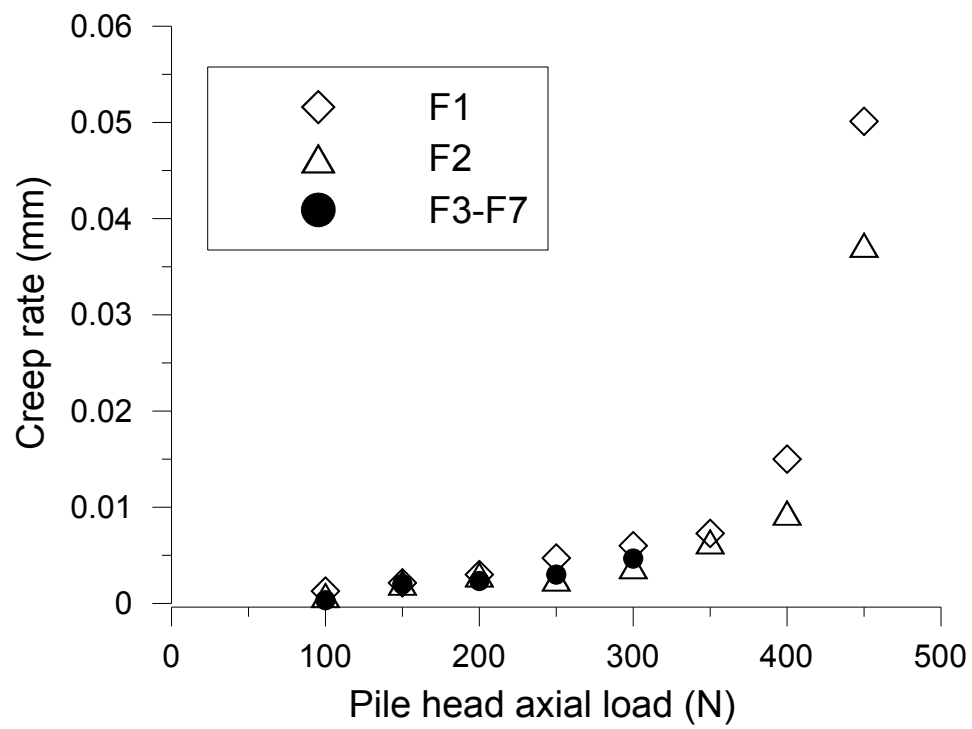


Figure 7. Creep rate versus axial load for the mechanical phase

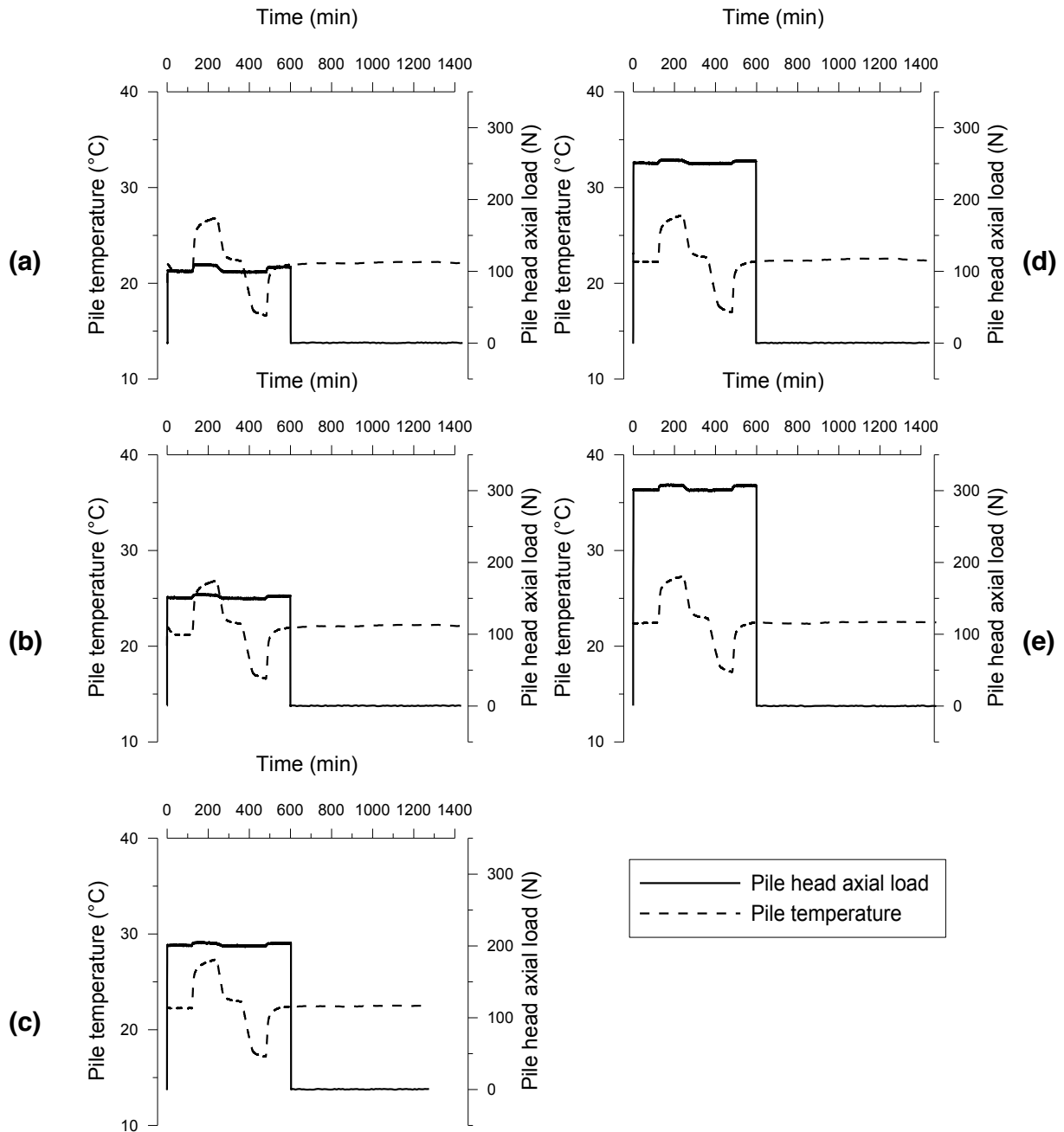


Figure 8. Axial load and temperature of the pile in tests: (a) F3; (b) F4; (c) F5; (d) F6; (e) F7.

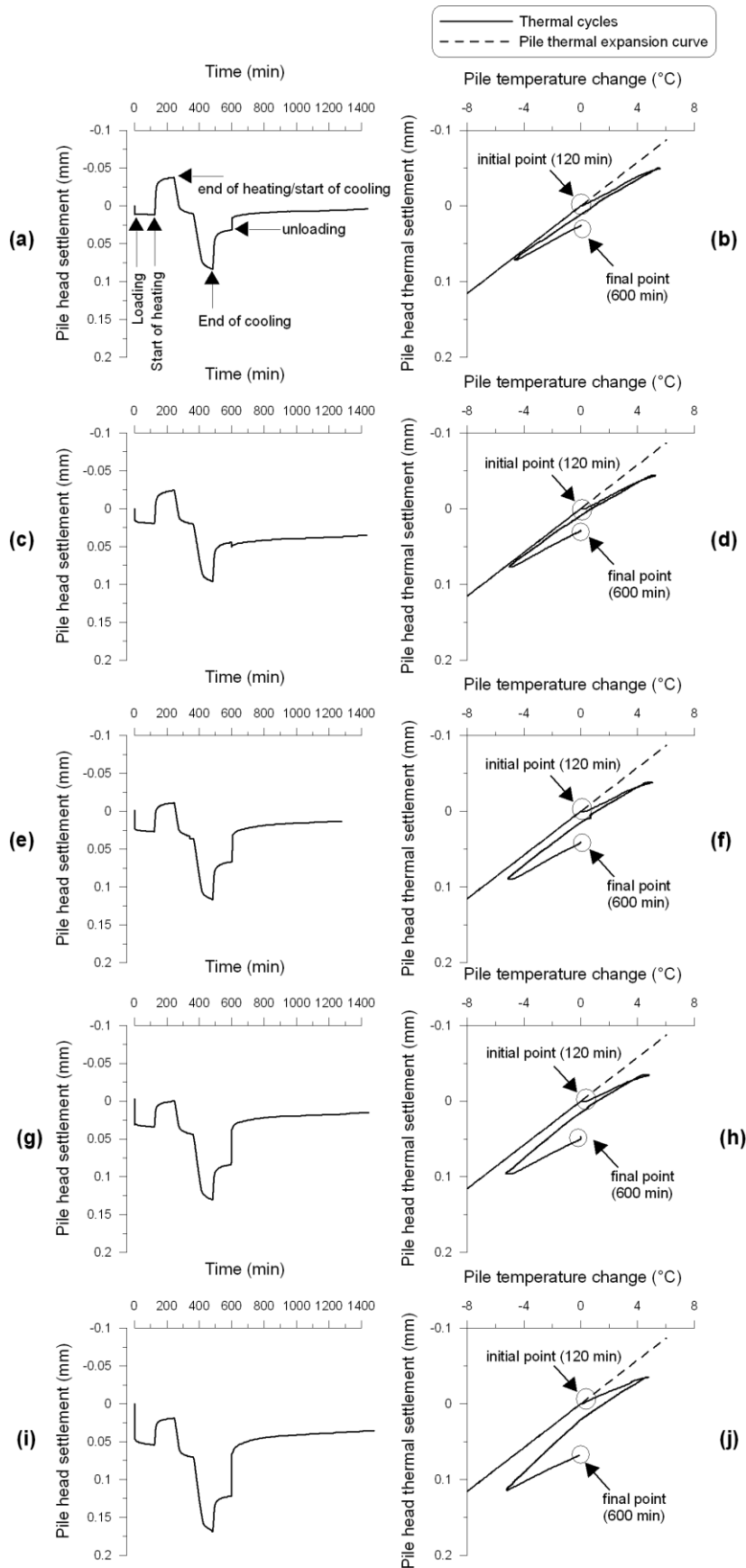


Figure 9. Results of tests F3-F7 for the thermal phase – Pile head settlement and pile temperature change: (a, b) F3; (c, d) F4; (e, f) F5; (g, h) F6; (i, j) F7.

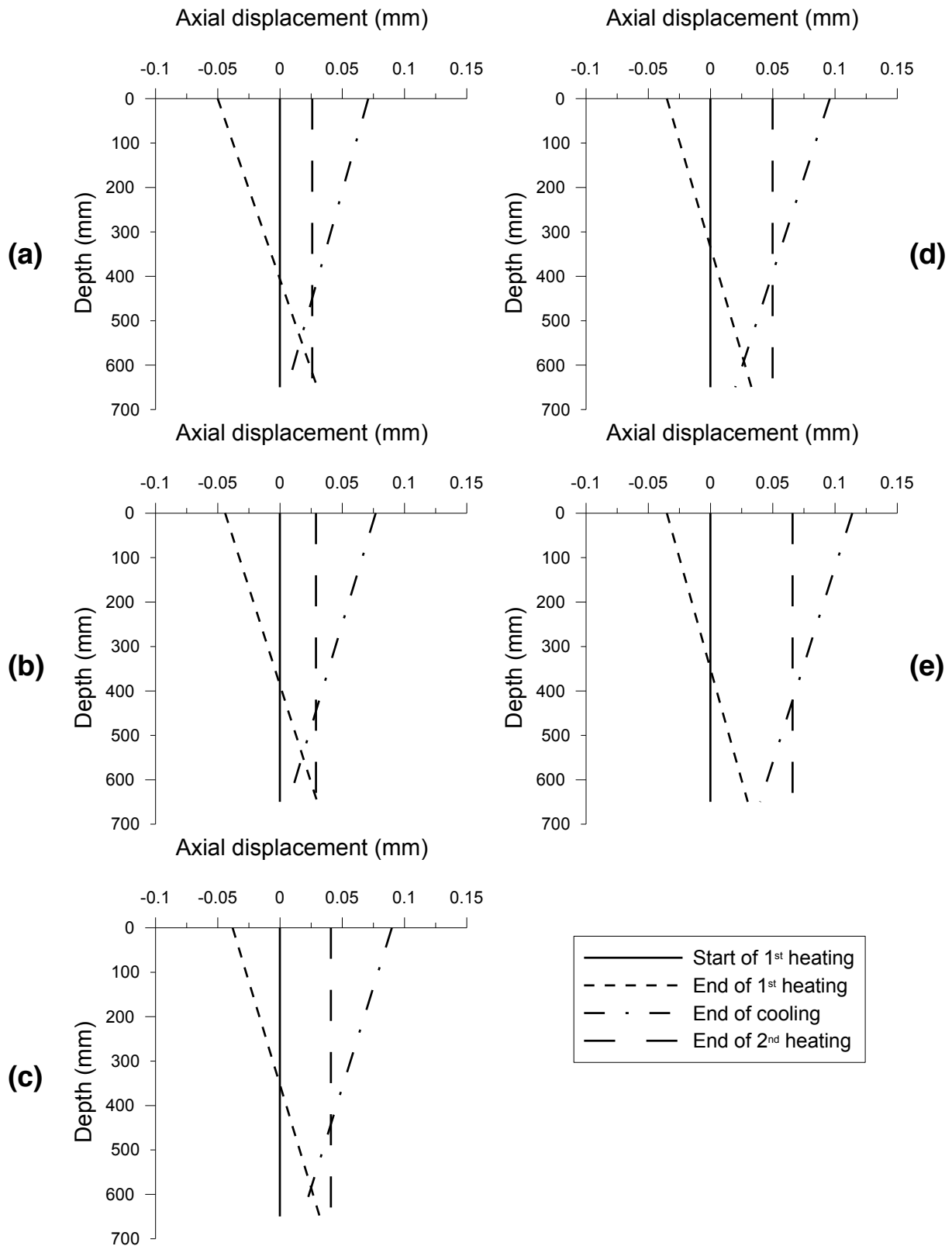


Figure 10. Results of tests F3-F7 for the thermal phase - Estimated axial displacement along the pile: (a) F3; (b) F4; (c) F5; (d) F6; (e) F7.

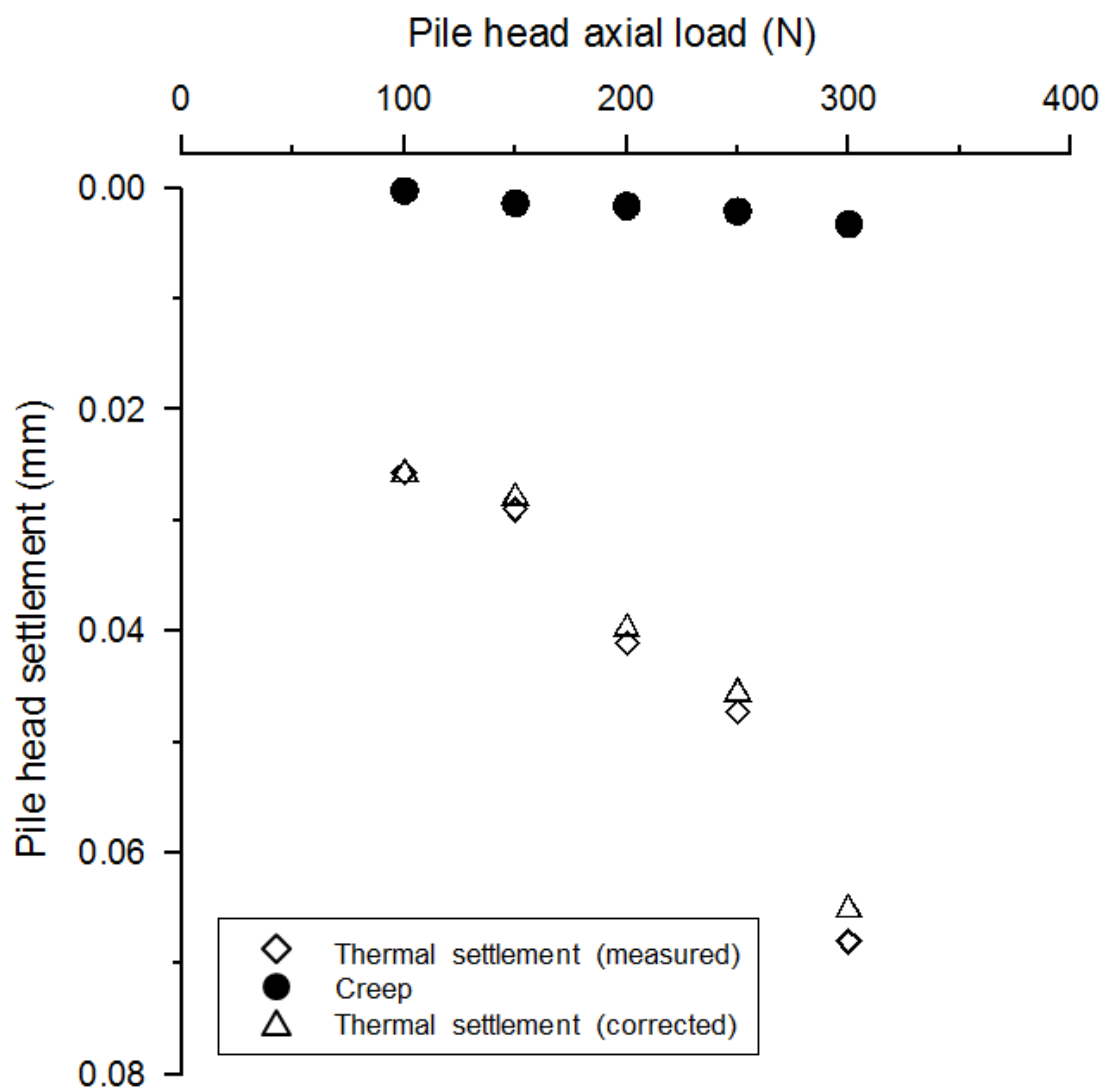


Figure 11. Results of tests F3-F7 for the thermal phase - Pile head settlement versus pile head axial load